TIJMET, Vol. 002 (2019) 16-24

The International Journal of

Materials and Engineering Technology

ISSN: 2667-4033
TIJMET ID: 190201003 (9 pages)
Type of the Paper: Article
Received 30.01.2019 Revised: 28.02.2019 Accepted: 18.03.2019 Published (Online): 13.03.2019
Journal homepage: http://dergipark.gov.tr/tijmet

APPLICATION OF FSW TECHNIQUE TO AA2124/%25SiCp-T4 ALUMINUM MATRIX COMPOSITES

HALIL IBRAHIM KURT[*1], YAHYA BOZKURT[2], SERDAR SALMAN[2] and HUSEYIN UZUN[3]

[1]Department of Mechanical and Metal Techomology, Gaziantep University, 27310, Gaziantep, Turkey
[2]Department of Metallurgy and Materials Engineering, Faculty of Technology, University of Marmara, 34722, Istanbul, Turkey
[3]Department of Metallurgy and Materials Engineering, Faculty of Technology, University of Sakarya, 54187, Sakarya, Turkey
E-mail:hiakurt@gmail.com

Abstract

In the present study, AA2124/25%vol.SiCp-T4 aluminum metal matrix composite plates were successfully friction stir butt joined using various welding parameters. The influence of the welding parameters on the temperature distribution, micro-hardness and tensile strength of the joints was investigated and the joint efficiency was determined. The temperature measurements were obtained from four points at the each side of the weld, namely tool advancing and tool retreating side, from the 15 mm away from the weld center. Based on these measurements, the average peak temperature in the weld nugget was predicted according to studies in literature. As a result of the study, the temperature dissipation shows that the maximum 180-270 °C occurred at 15 mm away from the centerline of the weld. The maximum and minimum values of joint performance was obtained at 1400/40 and 1400/100 rpm/min welding parameters as 73% and 59.32%, respectively. It was not detected a noticeable differences in micro-hardness measurements of the stir zone. It is determined that micro-hardness distribution in stir zone is in accordance with literature results which can be attributed to dynamic recrystallization.

Keyword: Friction stir welding, metal matrix composite, temperature dissipation, welding parameters.

1.Introduction

Metal matrix composite materials reinforced ceramic particle are especially used in aerospace industry due to its low cost, high wear resistance and high thermal stability. Aluminum and SiC are one of the most preferred materials as the matrix and reinforcing materials, respectively. Aluminum has a density of 2.7 gr/cm^3 and SiC particles are both cheap and wettable by aluminum that improve the preferability [1].

Appropriate application of welding technique to metal matrix composites (MMC) requires modern engineering technologies. Thus, fast production with high quality and economical can be done by welding process. Besides, it is very important to determine the most suitable welding method and welding parameters in joints. Because the welding parameters affect the physical and metallurgical properties of the joints, and therefore the quality of the welding [2]. Aluminum matrix reinforced particle composite materials when combined with conventional melting welding techniques like TIG, MIG, electron beam, laser etc., microstructural errors are encountered in the welding areas, which are detrimental to mechanical properties [3,4]. SiC reinforced composites have particularly some welding problems such as particle segregation in fusion welding processes, unwanted matrix-reinforcement reactions such as fragile Al_4C_3 phase, shrinkage during caking, oxide residues and gas cavities. In particular, the formation, size and shape of the Al_4C_3 phase are directly proportional to the heat input. The phase is stated to reduce the tensile strength, ductility and corrosion resistance of the weld [4,5]. Composite materials are successfully combined with friction stir welding (FSW), which is a solid-state welding technique and carried out under the melting temperature of the matrix that not use additional filler metal [6-9]. FSW technique has several advantages, such as low distortion and low welding temperature, compared to conventional melting welding methods. The materials to be joined by this method are connected with the fastening elements. Then, a rotating shoulder tool with a stirring tip and rotating at different speeds is contacted with the materials. The tip is slowly immersed in the material and the surfaces of the material soften with the effect of the heat generated by the friction. The process is carried out as the stirring tip is moved along the welding line and the softening material is stirred together [10].

In the literature, some works are carried out about FSW of Al alloys and Al matrix composites. Prado, Marzoli et al., [11,12], Mahyar et al., [13] and Feng and Ma, 6061 welded and investigated the microstructural and mechanical properties of Al alloy with Al_2O_3 20%, Al-Al_2O_3-B_4C plates and Al 2009 reinforced SiC 15% MMC [14]. They discussed the effect of process parameters on the microstructure and mechanical properties of joints.

In the friction stir welding, the temperature distribution in and around the stir zone affects the microstructure and mechanical properties of the welding. However, it is very difficult to clearly determine the temperature measurements in the stir zone. Therefore, during the FSW, the maximum temperatures at the stir zone are either estimated from the source microstructure or determined by the help of thermocouples embedded in a region close to the rotating stirring tip [10]. It has been determined that there is still no sufficient information in the literature about the combination of the 25% SiC particle reinforced AA2124 MMC materials, which are widely used in the aircraft industry, using different welding parameters by FSW method, determining the temperature distribution of the welds of the joints and the effects of these interactions on the hardness and strength properties. For this purpose; It is aimed to make experimental studies about the combinability of AA2124 MMC materials reinforced with 25% SiC particles, the temperature distribution around the weld and the mechanical properties of the weld zone.

2.Experimental Method

In this study, AA2124/SiCp/25-T4 MMC plates are welded by FSW technique. MMCs are available as billet with measuring 400x260x50 mm^3. The billet that is available in dimensions of 400x260x50 mm^3 is cut into 130x50x3 mm^3 with the wire erosion at the tool feed speed of 2 mm / min. In order to determine the temperature distribution during welding, blind holes are placed on the plates to place thermocouples. Table 1 shows the compositions, the tensile and hardness properties of the used material. In the FSW process, the tool produced from 1.334 high speed steel (HSS) with a shoulder diameter of 20 mm is used. The FSW tool is reached a hardness value of 62 HRC with quenching heat treatment. The joining process was performed as the universal vertical milling machine with the welding parameters shown in Table 2.

.

Table 1. Compositions (wt.%) and mechanical properties of the plate

Material	Cu	Mg	Mn	Si	Al	UTS (MPa)	Hardness (HV)
	3.86	1.52	0.65	0.17	Reaminder	454	190

During the FSW, thermocouples of K type data readers with 8-point (capable of measuring between -200 and 1372 ° C) are placed on the plates and the temperature distribution was determined. The layout of the thermocouple during the FSW is shown in Figure 1. The thermocouples are located at 10, 45, 85 and 120 mm distances to the blind holes opening 3 mm in diameter and 2 mm deep to the distances 15 mm away from tool advancing side (AS) and tool retreating side (RS) of the plates (Fig.1). Figure 2 also displays FSW device.

Table 2. Welding parameters used in friction stir welding

Tool rotational speed (rpm)	Tool traverse speed (mm/min)	Tilting angle	Tool rotational direction
355	40 50	2º	Clockwise
1400	80 100		

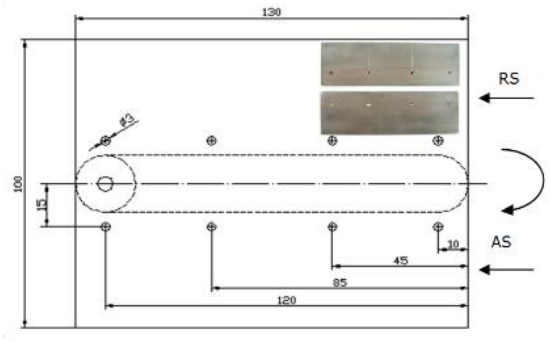

Figure 1. Thermocouple layout as schematic

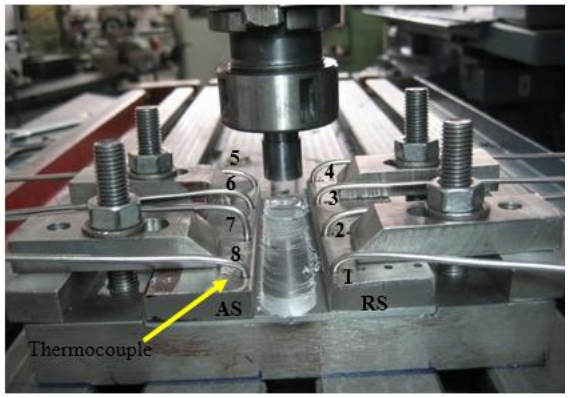

Figure 2. Friction stir welding device and test fixture with thermocouples

Tensile test specimens are prepared in CNC controlled milling machine with numerical control using a 1.9 mm diameter carbide milling. Tensile tests are made in Zwick Z010 universal type device. 3 samples were tested for each experiment and the results were determined by taking the average. The microhardness of the samples taken at 1 mm intervals from the lower and upper parts of the FSW method was determined by using the Vickers hardness (HV) method. Measurements were made by using Schimadzu brand micro hardness tester of type M with 30 sec. Welding performance (WP) was determined by the ratio of tensile strength (σ_t) of the welded specimens combined with SSK to tensile strength (σ_a) of the base metal (Eq. 1).

(%) WP = (σt (MPa) / σa (MPa)) x 100 (1)

3.Results

The temperature distribution of the joints obtained by the friction stir welding process is shown in Figure 3. As can be seen from this figure, the temperature distribution at a distance of 15 mm from welding zone of the AA2124/SiCp/25-T4 MMC sheets joined at tool rotational and traverse speeds of 355-1400 rpm and 40-100 mm/min varies between 180-270 °C. This temperature range is much lower than the melting point of aluminum (660°C) and it is equivalent to the recrystallization temperature of the aluminum matrix. Therefore, it can be said that the joining process is carried out by the plastic deformation mechanism and the mixing of the plates.

The tensile test was performed to determine the joining strength and weld performance of the MMC plates combined with the FSW. As shown in Figure 4, the ultimate tensile strengths (UTS) and weld performances (WP) of 355/40, 355/100, 1400/40 and 1400/100 the joints are 300.09, 278.30, 331.42 and 269,31, MPa and 66.10%, 61.30%, 73.00% and 59.32%, respectively. The maximum tensile strength and welding performance are obtained with welding parameters of 1400/40 (tool rotational speed of 1400 rpm and tool traverse speed of 40 mm/min) as 331.42 MPa and 73.00%, respectively. The minumum tensile strength and welding performance are obtained with welding parameters of 1400/100 as 269.31 MPa and 59.320%, respectively. Figures 5 illustrates the fractured surface of FSW joints with welding parameters of 355/40-100 and 1400/40-100 after tensile test. It is clear that the joints with welding parameter of 355/40-100 faractured from HAZ of AS whereas the joints with welding parameter of 1400/40-100 fractured from stir zone that can be attributed to microstructure variables and particulate distrubution.

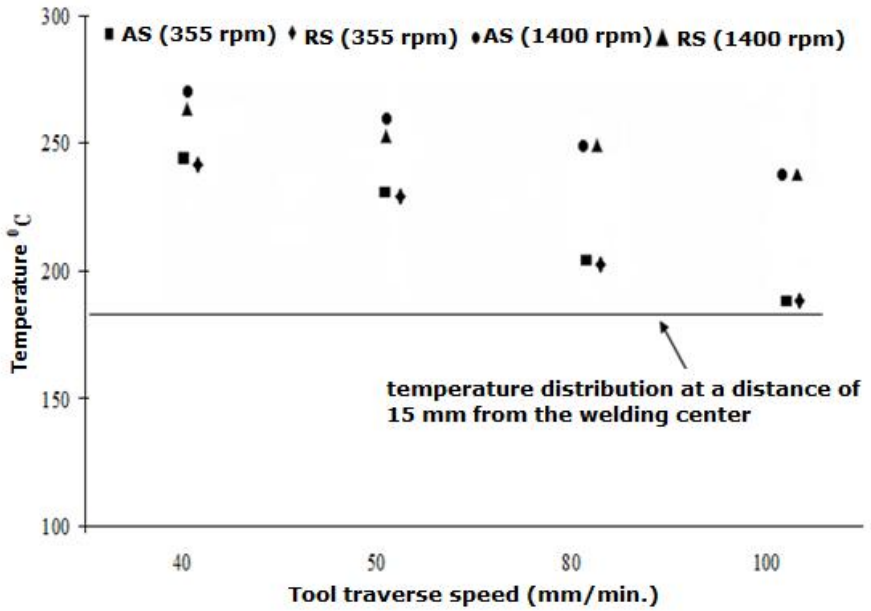

Figure 3. Temperature dissipation of FSW joint at different tool rotation and transverse speeds

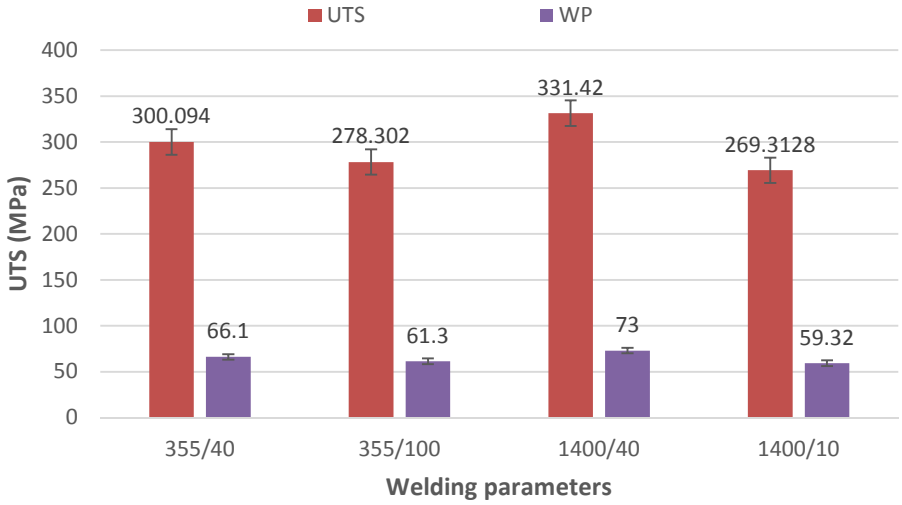

Figure 4. Tensile test results

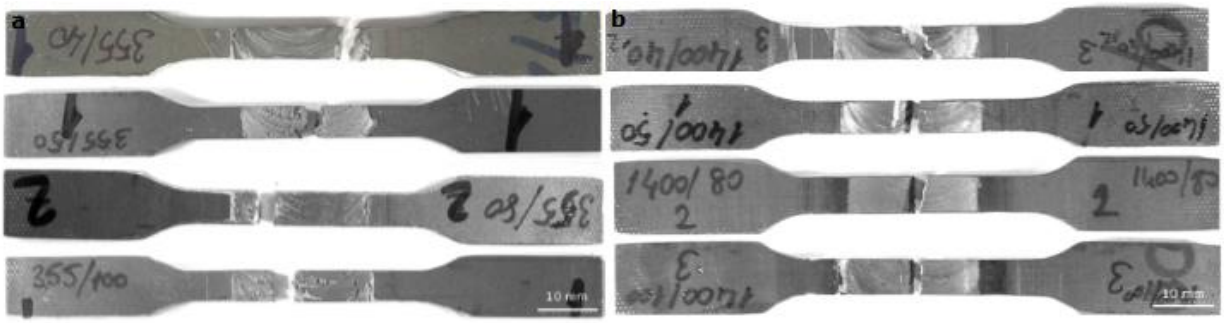

Figure 5. Cracked surface appearance of FSW after tensile test a) 355/40-100 b)1400/40-100

Figures 6 and 7 show the microhardness distribution of the samples obtained with welding parameters 1400/40 and 1400/100 where maximum and minimum welding performance values are obtained. The hardness of AA2124/SiCp/25-T4 composite plates showed the increase by the rise of the tool rotation and traverse speeds. When the tool rotation speed increases for 40 and 100 mm/min, hardness decreases as tool rotation speed increases. The hardness values of the base metal and FSW joints were determined to vary between 140-235 $HV_{0.2}$.

Figure 8 shows the microstructure images of the stir zones of the composites which combine with different process parameters.

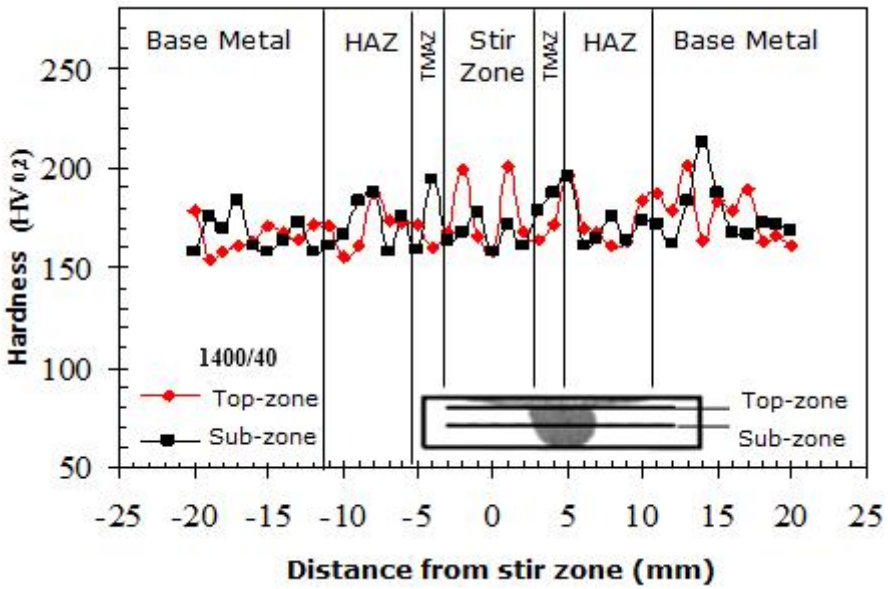

Figure 6. The microhardness graph measured from the top and bottom zone for 1400/40 welding parameters

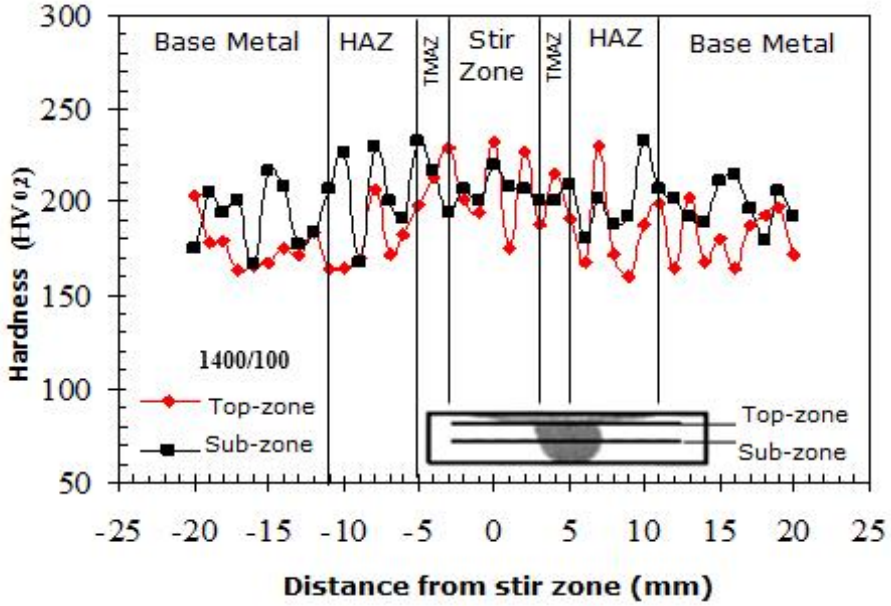

Figure 7. The microhardness graph measured from the top and bottom zone for 1400/100 welding parameters

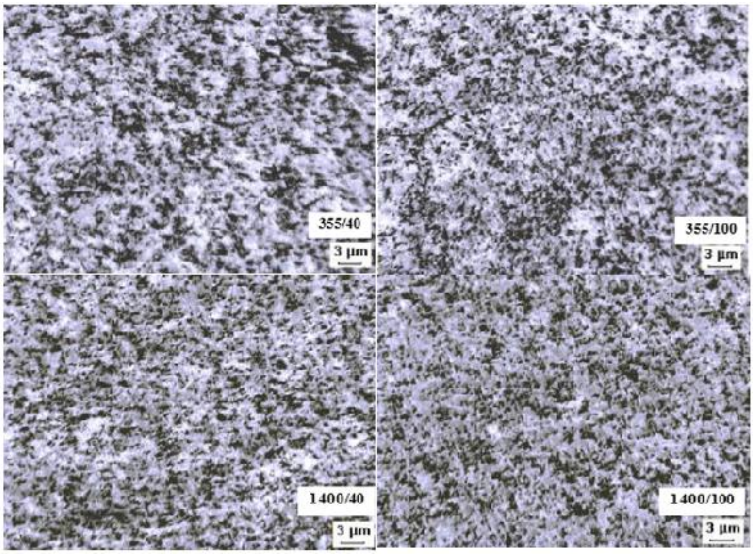

Figure 8. The microstructure images of stir zones

It has been observed that the materials have a good mixture with different welding parameters. The distribution of the matrix and secondary phases is relatively good. The stir region of the sample combined with 1400/40-100 experimental parameters exhibits finer grain structure due to dynamic recrystallization. Significant microstructure changes such as reduction of heterogeneity, redirection of reinforcing particles and microstructural anisotropy are observed during the friction stir welding. The effects such as agglomeration, grain growth, particle roughening and dissolution, porosity etc. depending on the welding parameters and temperature cause a decrease in mechanical properties [15-17].

4.Discussion

The temperature distribution in the stir zone and its surrounding causes the change of factors such as grain size, grain boundary, precipitation dissolution and coarsening, which affect the welding microstructure and mechanical properties [18]. However, the measurement of temperature in the stir zone can be determined using various models and predictions is very difficult due to the intense plastic deformation caused by the rotation and movement of the tool. The temperature decreased as it moved away from the stir zone. The temperature at the edge of the stir zone increases from the bottom surface of the plate to the upper surface. The temperature is believed to exceed the temperature of the solution for precipitation hardening in the aluminum alloy. Therefore, the maximum temperatures occurring in the stir zone during FSW are either estimated from the source microstructure or determined by the help of the thermocouple embedded in a region close to the rotating stir tip. The welding temperature of the 7075-T651 alloy was estimated at about 400-480 °C and the temperature of the Al 6061 alloy was 400°C [16,19]. Temperature values of 8.5, 10, 12.5 and 15 mm distances from the welding center were obtained as 402, 353, 302 and 201 °C, respectively, by comparing the microstructures of similar welding thermal cycles at different maximum temperatures [20]. The increase in the distance decreases the temprerature. The previous thermal models of the FSW were determined by using the classical Rosenthal equation [21]. This equation describes an almost stable state of temperature in a semi-infinite environment through a heat source point moving at a constant speed. These models are considered as the heat generated by the friction work at the shoulder-plate interface, thus it is prevented the friction heat at the plastic energy distribution and the agitator end-workpiece interface. There is a uniform force on the entire contact surface obtained by friction. The temperature measurements described in the studies were obtained by placing the thermocouples thoroughly and there was no temperature and any melting sign above 0.8 T_m. Marzoli et al. 20% Al_2O_3 particle-reinforced AA 6061-T6 MMCs are FSWelded. Thermocouples of type K of 6 are placed at a distance of 15 mm of welding zone with a distance of 10 mm on AS, and temperatures were reported to be around 190-255 °C [12]. Covington [22] welded the Al 7075-T7351 alloy by FSW and examined the amount of heat on tool. The heat in shoulder region is 79%, it is 20% in the beginning of the stir tip and is 1% in the stir tip. It is stated that during FSW, temperature in the stir region is between 371-507 °C. Similar studies on the determination of temperature distributions have been made in the literature and the results of our study coincide with the literature results [19,23].

The tensile strength and joining efficiency of joints were analyzed. Reduction in tensile strength and joining efficiency resulted in increasing tool tarverse speed (40-100 mm / min) for tool rotational speed of 355 rpm). Similarly, the tensile strength and joining efficiency for 1400 rpm were reduced with increasing tool feed speed. Maximum tensile strength (330.75 MPa) and joining efficiency (73%) were obtained at a tool rotation speed of 1400 rpm and a tool traverse speed of 40 mm/min. Lower tensile strength and welding efficiency can be attributed to the formation of coarser grain structure in HAZ that was stated in the previous study [17]. Dynamic recrystallization occurs as a result of plasic deformation in FSW method and SiC particles significantly affect dynamic recrystallization. Dynamic recrystallisation occurs in the regions with high dislocation density. In other words, SiC particles provide more nucleation sites for new crystallizing grains by increasing regional stress in the matrix and modifying lattice orientation [24]. The microhardness tests were performed in different regions. The hardness properties depend mainly on the state of the precipitates and due to the coarsening and excessive aging of the precipitates, especially in the heat-affected zone and in the thermomechanically affected region (TMAZ). The decrease in the hardness was reported and it was found that there was a softening of the base metal for similar reasons in the mixture zone [25,26]. The matrix-SiC interface is affected from the thermal expansion, rapid heating and cooling [27]. However, in this study, no significant difference was observed in the hardness values of the base metal. Welding parameter of 1400/40 is more homogenous than welding parameter of 1400/100 and the deformation caused by the severe stir movement results in a decrease in the size of the SiC particles, especially in the TMAZ in the RS, starting from the mixing zone. As a result, it can be said that the hardness change in the mixture region is due to the re-crystallized grain structure.

In Al-Cu-Mg alloys, solid solution precipitation, grain refinement, (Al_2Cu) and S (Al_2MgCu) particle formation are the important phases that provide strength increase. With the addition of a reinforcemnet, the density of dislocation, the thermal incompatibility and the load transfer mechanism play an important role in the increase of strength and the coarsening of these phases with heat reduces the hardness and tensile strength [28-30]. The friction between the tool and the workpieces produces intense plastic deformation around the rotating tool. Both of these factors cause to increase the temperature in and around the stir zone. It is very important to investigate the thermal cycle and thermal dispersion of metallurgical transformations and to determine the ratio of these transformations. During the welding process, moves of the tool causes more heat to develop in the direction of this [31]. In the stir zone, higher stiffness can be attributed to the formation of thinner grains as a result of dynamic recrystallization [32]. It is also important to determine the effect of each factor such as the distribution, size, morphology and dissolution of the particles in detail. It is reported to be completely dissolved of precipitates into the Al 6063 alloy (0 - 8,5 mm from the welding center) [20] and not dissolves of some precipitates in welding zone [16]. The re-precipitation and dissolution of larger precipitates in a study on the microstructural development of the FSW in the Al 7075-T651 alloy were found in the welding center [19].

5.Conclusion

AA2124/SiCp /25-T4 MMC plates are successfully joined with the FSW technique both low and high tool rotation speeds. It was determined that the temperature distribution at 15 mm distance from the welding center varied between 180-270 °C at tool rotational speeds of 355-1400 rpm and tool traverse speeds of 40-100 rpm. According to the studies in the literature, it can be said that the temperature in the mixture zone is around 450-500 °C. Temperature increases with constant tool feed speed and increased tool rotation speed. If the tool rotation speed is kept constant and the feed rate is increased, the temperature decreases. The highest temperature rise occurs on the top surface of the welding zone. The welding performance performed at welding parameters of 355/40-100 and 1400/40-100 was determined as maxiumum 73% with 1400/40 welding parameters and as minimum 59% with 1400/100 welding parameters. The microhardness distributions within the weld zone were found to be significantly close to each other.

References

1. Chawla, N.; Chawla, K. Metal-matrix composites in ground transportation. *JoM* **2006**, *58*, 67-70.
2. Kurşun, T. Gazaltı kaynak tekniğinde kullanılan koruyucu gaz ve gaz karışımlarının 19mn6 kalite çeliğinin kaynatılmasında mekanik özelliklere etkisi ve tozaltı kaynağı ile karşılaştırması. *Erciyes Ünv. Fen Bil. Ens., Yüksek Lisans Tezi, Kayseri* **1998**.
3. Ellis, M. Joining of aluminium based metal matrix composites. *International Materials Reviews* **1996**, *41*, 41-58.
4. Urena, A.; Escalera, M.; Gil, L. Influence of interface reactions on fracture mechanisms in tig arc-welded aluminium matrix composites. *Composites Science and Technology* **2000**, *60*, 613-622.

5. Rotundo, F.; Ceschini, L.; Morri, A.; Jun, T.-S.; Korsunsky, A. Mechanical and microstructural characterization of 2124al/25 vol.% sicp joints obtained by linear friction welding (lfw). *Composites Part A: Applied Science and Manufacturing* **2010**, *41*, 1028-1037.
6. Wert, J.A. Microstructures of friction stir weld joints between an aluminium-base metal matrix composite and a monolithic aluminium alloy. *Scripta Materialia* **2003**, *49*, 607-612.
7. Fernandez, G.; Murr, L. Characterization of tool wear and weld optimization in the friction-stir welding of cast aluminum 359+ 20% sic metal-matrix composite. *Materials Characterization* **2004**, *52*, 65-75.
8. Ceschini, L.; Boromei, I.; Minak, G.; Morri, A.; Tarterini, F. Microstructure, tensile and fatigue properties of aa6061/20 vol.% al2o3p friction stir welded joints. *Composites Part A: Applied Science and Manufacturing* **2007**, *38*, 1200-1210.
9. Minak, G.; Ceschini, L.; Boromei, I.; Ponte, M. Fatigue properties of friction stir welded particulate reinforced aluminium matrix composites. *International Journal of Fatigue* **2010**, *32*, 218-226.
10. Uzun, H.; Dalle Donne, C.; Argagnotto, A.; Ghidini, T.; Gambaro, C. Friction stir welding of dissimilar al 6013-t4 to x5crni18-10 stainless steel. *Materials & design* **2005**, *26*, 41-46.
11. Prado, R.; Murr, L.; Shindo, D.; Soto, K. Tool wear in the friction-stir welding of aluminum alloy 6061+ 20% al2o3: A preliminary study. *Scripta materialia* **2001**, *45*, 75-80.
12. Marzoli, L.; Strombeck, A.; Dos Santos, J.; Gambaro, C.; Volpone, L. Friction stir welding of an aa6061/al2o3/20p reinforced alloy. *Composites Science and Technology* **2006**, *66*, 363-371.
13. Mohammadnezhad, M.; Shamanian, M.; Zabolian, A.; Taheri, M.; Javaheri, V.; Navidpour, A.H.; Nezakat, M.; Szpunar, J.A. Microstructure and crystallographic texture variations in the friction-stir-welded al-al 2 o 3-b 4 c metal matrix composite produced by accumulative roll bonding. *Metallurgical and Materials Transactions A* **2015**, *46*, 5747-5755.
14. Feng, A.; Ma, Z. Formation of cu2feal7 phase in friction-stir-welded sicp/al–cu–mg composite. *Scripta Materialia* **2007**, *57*, 1113-1116.
15. Jata, K.; Semiatin, S. *Continuous dynamic recrystallization during friction stir welding of high strength aluminum alloys*;: 2000.
16. Liu, G.; Murr, L.; Niou, C.; McClure, J.; Vega, F. Microstructural aspects of the friction-stir welding of 6061-t6 aluminum. *Scripta materialia* **1997**, *37*, 355-361.
17. Xie, G.; Ma, Z.; Geng, L. Development of a fine-grained microstructure and the properties of a nugget zone in friction stir welded pure copper. *Scripta Materialia* **2007**, *57*, 73-76.
18. Milagre, M.X.; Mogili, N.V.; Donatus, U.; Giorjão, R.A.R.; Terada, M.; Araujo, J.V.S.; Machado, C.S.C.; Costa, I. On the microstructure characterization of the aa2098-t351 alloy welded by fsw. *Materials Characterization* **2018**, *140*, 233-246.
19. Rhodes, C.; Mahoney, M.; Bingel, W.; Spurling, R.; Bampton, C. Effects of friction stir welding on microstructure of 7075 aluminum. *Scripta materialia* **1997**, *36*, 69-75.
20. Sato, Y.S.; Kokawa, H.; Enomoto, M.; Jogan, S. Microstructural evolution of 6063 aluminum during friction-stir welding. *Metallurgical and Materials Transactions A* **1999**, *30*, 2429-2437.
21. Russell, M.J.; Shercliff, H.R. In *Analytical modeling of microstructure development in friction stir welding*, 1. International Symposium on Friction Stir Welding, Thousand Oaks, Cal, USA, 1999; Thousand Oaks, Cal, USA.
22. Covington, J.L. Experimental and numerical investigation of tool heating during friction stir welding. **2005**.
23. Vilaça, P.; Quintino, L.; dos Santos, J.F.; Zettler, R.; Sheikhi, S. Quality assessment of friction stir welding joints via an analytical thermal model, istir. *Materials Science and Engineering: A* **2007**, *445*, 501-508.
24. Nandipati, G.; Damera, N.; Nallu, R. Effect of microstructural changes on mechanical properties of friction stir welded nano sic reinforced aa6061composite. *International Journal of Engineering Science and Technology* **2010**, *2*, 6491-6499.
25. Sivaraj, P.; Kanagarajan, D.; Balasubramanian, V. Effect of post weld heat treatment on tensile properties and microstructure characteristics of friction stir welded armour grade aa7075-t651 aluminium alloy. *Defence Technology* **2014**, *10*, 1-8.
26. Bozkurt, Y.; Uzun, H.; Salman, S. Microstructure and mechanical properties of friction stir welded particulate reinforced aa2124/sic/25p–t4 composite. *Journal of Composite Materials* **2011**, *45*, 2237-2245.
27. Adesina, A.Y.; Al-Badour, F.A.; Gasem, Z.M. Wear resistance performance of alcrn and tialn coated h13 tools during friction stir welding of a2124/sic composite. *Journal of Manufacturing Processes* **2018**, *33*, 111-125.
28. Miller, W.S.; Humphreys, F.J. Strengthening mechanisms in particulate metal matrix composites. *Scripta Metallurgica et Materialia* **1991**, *25*, 33-38.

29. Embury, J.D.; Lloyd, D.J.; Ramachandran, T.R. 22 - strengthening mechanisms in aluminum alloys. In *Treatise on materials science & technology*, Vasudevan, A.K.; Doherty, R.D., Eds. Elsevier: 1989; Vol. 31, pp 579-601.
30. Shaterani, P.; Zarei-Hanzaki, A.; Fatemi-Varzaneh, S.M.; Hassas-Irani, S.B. The second phase particles and mechanical properties of 2124 aluminum alloy processed by accumulative back extrusion. *Materials & Design* **2014**, *58*, 535-542.
31. Donatus, U.; Thompson, G.E.; Zhou, X.; Wang, J.; Beamish, K. Flow patterns in friction stir welds of aa5083 and aa6082 alloys. *Materials & Design* **2015**, *83*, 203-213.
32. Gao, C.; Zhu, Z.; Han, J.; Li, H. Correlation of microstructure and mechanical properties in friction stir welded 2198-t8 al–li alloy. *Materials Science and Engineering: A* **2015**, *639*, 489-499.